Research Article | Vol. 29, No. 1 / 4 January 2021 / Optics Express 359

Optics EXPRESS

High-resolution beam scanning technique with microlens array and adaptive fiber-optics collimator

Xu Yang,[1,2,3,4] **Chao Geng,**[1,3,5] **Feng Li,**[1,3] **Xiaoyang Li,**[1,2,3,4] **Jing Zuo,**[1,3,4] **Jiali Jiang,**[1,3] **Bincheng Li,**[2] **and Xinyang Li**[1,3,6]

[1] *Key Laboratory on Adaptive Optics, Chinese Academy of Sciences, Chengdu 610209, China*
[2] *School of Optoelectronic Science and Engineering, University of Electronic Science and Technology of China, Chengdu 610054, China*
[3] *Institute of Optics and Electronics, Chinese Academy of Sciences, Chengdu 610209, China*
[4] *University of Chinese Academy of Sciences, Beijing 100049, China*
[5] *blast_4006@126.com*
[6] *xyli@ioe.ac.cn*

Abstract: Conventional beam scanning systems employing a microlens array (MLA) suffer from the problem that only discrete diffraction angles can be addressed because of the periodic structure of the MLA. In this paper, an adaptive fiber-optics collimator (AFOC) that continuously adjusts the position of light source (optic fiber output) is used in front of the periodic structure as a moving linear phase shifter to overcome this discrete scanning angle problem. By introducing the AFOC into the beam scanning system employing MLA, a beam scanning system with continuous scanning capability and high resolution is fulfilled. Theoretical simulations and experimental results both demonstrate the continuous high-resolution scanning capacity of the beam scanning system employing both MLA and AFOC. The proposed beam scanning system is expected to find wide applications in space optical communication, optical interconnection, power projection, and coherent beam combining.

1. Introduction

Today, fast and accurate beam scanning enables applications such as optical communication and power projection. Considerable efforts have been focused on the development of beam scanning devices with compact structure, low weight, high agility, and large field of regard [1–3]. Potentially, such beam scanning devices can be realized with the employment of microlens array (MLA) [4–6]. Due to the small size of the lenslets in MLA, large scan angle ranges can be achieved by small offsets and large apertures can be realized by increasing the number of the lenslets.

Normally, beam scanning systems employing MLAs are basically telescopic array systems. Three telescopic array arrangements, that are, Galilean structure [4], Keplerian structure [5] and optimized Keplerian structure [6], are used in the MLA based beam scanning systems. In such structures, the MLAs work as the blazed grating. According to the nature of blazed grating, only discrete scanning angles can be addressed. The beam can be scanned from one diffraction order to the adjacent diffraction order in a discrete way, therefore limit the scanning capacity of the MLA based beam scanning systems. Comb actuators [7] and piezoelectric actuators [8] can be used to drive the MLA with high frequency.

Beam scanning into arbitrary angles (that is, with continuous scanning capability) can be achieved by tilting the incident wavefront using a movable field lens before the beam entering the blazed grating formed with MLAs. Constructive interferences can be satisfied by the offset

#412272
Journal © 2021
https://doi.org/10.1364/OE.412272
Received 13 Oct 2020; accepted 12 Dec 2020; published 23 Dec 2020

Optics EXPRESS

of the field lens [6]. However, the diameter of the field lens should equal to that of the MLAs, which causes a greater weight of the field lens. In this case the performance of the beam scanning system will be affected.

In this paper, we propose a solution to the discrete scanning problem while maintaining all the advantages of the MLA based beam scanning systems. In the proposed beam scanning system, an adaptive fiber-optics collimator (AFOC) is added before the MLAs as a pre-scanning device. The small angular deflection or coupling reception of the beam which is needed for continuous scanning can be realized by adjusting the lateral offset of the fiber tip on the focal plane of the collimating lens in AFOC. In this arrangement, the AFOC is used to tilt the incident wavefront of the beam entering the MLAs. Compared with the moving field lens approach [6], the moving fiber tip method proposed in this paper is much faster and more agile.

The beam scanning systems employing MLA and AFOC can find applications in laser coherent beam combining and laser communication [9,10]. For AFOCs, the production and applications were intensely investigated in our laboratory in recent years [11,12].

This paper is structured as follows. In section 2, the optical arrangement of the continuous beam scanning system employing MLAs and AFOC is described and analyzed. In section 3 the experimental verification of continuous scanning capacity of the proposed beam scanning system is presented. Finally, the conclusion is drawn in section 4.

2. MLA and AFOC based beam scanning system

The optical arrangement of the proposed beam scanning system employing MLA and AFOC is illustrated in Fig. 1. In this arrangement the Keplerian structure is used. There are two parts in the proposed beam scanning system, one is the pre-scanning element (AFOC) consisting of a fiber tip and a collimating lens, and the other is the MLA element consisting of two convex MLAs. A far-field transform lens is used to get the far-field distribution of the scanning spot.

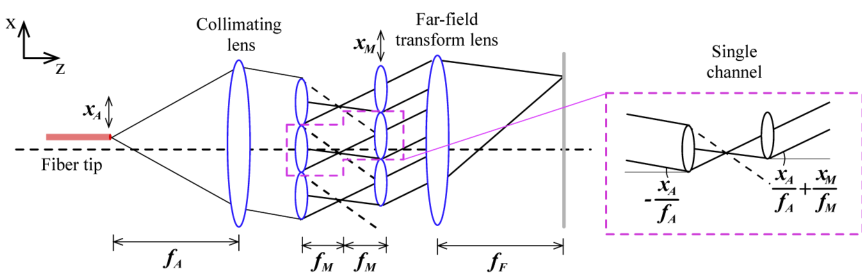

Fig. 1. Schematic diagram of the optical arrangement of the proposed beam scanning system employing MLA and AFOC. Continuous scanning is achieved by the relative displacements of MLAs and AFOC.

A tilting collimated beam caused by the offset of the fiber tip is used as the light source, the field distribution of beam emerging from the AFOC is expressed as:

$$u_1(x) = rect\left[\frac{x}{W_A}\right]\exp\left[-jk\frac{x_A}{f_A}x\right] \tag{1}$$

where W_A is the width of beam emitting from the AFOC, f_A is the focal length of the collimating lens in the AFOC, k is the wavenumber, and x_A is the offset of the AFOC fiber tip.

As shown in the subgraph of Fig. 1, ignoring the leakage light, the transmission function $t(x)$ of a single channel of the 2-MLAs is given by [13]:

$$t(x) = rect\left[\frac{x}{W_M\cdot ff}\right]\exp\left[jk\left(2\frac{x_A}{f_A}+\frac{x_M}{f_M}\right)x\right] \tag{2}$$

where W_M is the aperture size of the lenslet in the MLAs, f_M is the focal length of the MLAs, x_M is the relative displacement between the two MLAs, and $ff\,(0<ff \leq 1)$ is the effective optical filling factor. The relative displacement between the two sets of micro lenslets will cause a decrease in ff.

According to Fourier optics theory [14], the transmission function of the all 2-MLAs channels can be written as:

$$T(x) = \frac{1}{L} comb\left[\frac{x}{L}\right] \otimes t(x) \tag{3}$$

where L is the lens spacing of the MLAs. The symbol $\otimes$ represents convolution.

Accordingly, the field distribution of beam scanning system' emerging beam in the scanning direction can be written as:

$$\begin{aligned} u_2(x) &= u_1(x)T(x) \\ &= \left\{rect\left[\frac{x}{W_A}\right] exp\left[-jk\frac{x_A}{f_A}x\right]\right\} \times \left\{\frac{1}{L} comb\left[\frac{x}{L}\right] \otimes t(x)\right\} \end{aligned} \tag{4}$$

The field distribution at the far-field plane is obtained by the Fourier transform of $u_2(x)$:

$$\begin{aligned} I &= \left| sinc\left[W_A\left(f_x + \frac{x_A}{\lambda f_A}\right)\right] \otimes comb[f_x L]\right|^2 \\ &\quad \times \left| sinc\left[W_A \cdot ff\left(f_x - 2\frac{x_A}{\lambda f_A} - \frac{x_M}{\lambda f_M}\right)\right]\right|^2 \\ &= I_1 \times I_2 \end{aligned} \tag{5}$$

where f_x is the normalized far-field coordinate ($f_x = \frac{x}{\lambda f_F}$), f_F is the focal length of the far-field transform lens, $sinc\left[W_M \cdot ff\left(f_x - 2\frac{x_A}{\lambda f_A} - \frac{x_M}{\lambda f_M}\right)\right]$ is the energy envelope, $\left\{sinc\left[W_A\left(f_x + \frac{x_A}{\lambda f_A}\right)\right] \otimes comb[f_x L]\right\}$ is the diffraction order grid. Moving AFOC causes both the energy envelope and diffraction order grid to move in opposite directions. On the other hand, the motion of MLA causes only the movement of the centroid of the energy envelope, while the diffraction order grid keeps not moved. Thus, from Eq. (5) and Fig. 2, both the diffraction order gird and the energy envelope are scanned, ensuring a maximal scanned energy in any desired direction.

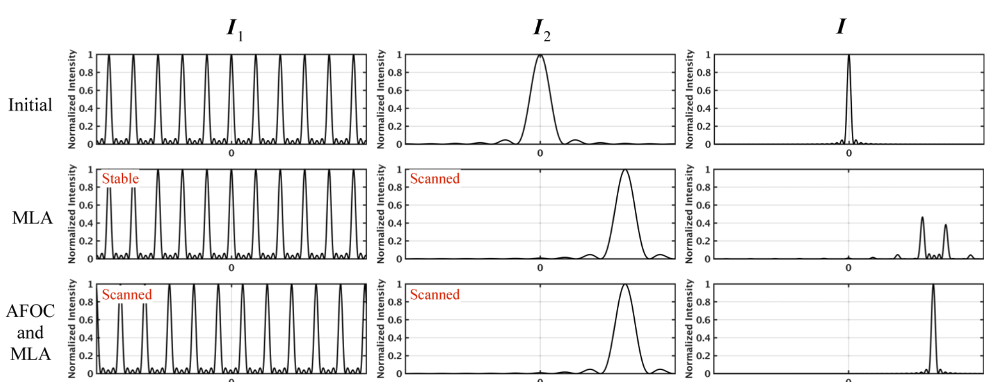

Fig. 2. The principle of the continuous scanning.

The total beam scan angle is expressed as:

$$\theta_T = \frac{x_A}{f_A} + \frac{x_M}{f_M} \tag{6}$$

An arbitrary scan angle θ_{T} can be achieved by choosing x_A and x_M subject to the following conditions:

$$x_A = (\frac{n\lambda}{L} - \theta_{\mathrm{T}})f_A, \quad n = 0, \ \pm 1, \ \pm 2 \ldots \tag{7}$$

$$x_M = (\theta_{\mathrm{T}} - \frac{x_A}{f_A})f_M \tag{8}$$

The angular separation of the diffraction order grid is:

$$\theta_{\mathrm{as}} = \frac{\lambda}{L} \tag{9}$$

The angular width of the scanning spot is:

$$\theta_{\mathrm{aw}} = \frac{2\lambda}{W_A} \tag{10}$$

Consequently, as shown in Fig. 3, the number of scanning spots that can be accommodated in one angular separation is:

$$N = \frac{W_A}{L} + 1 \tag{11}$$

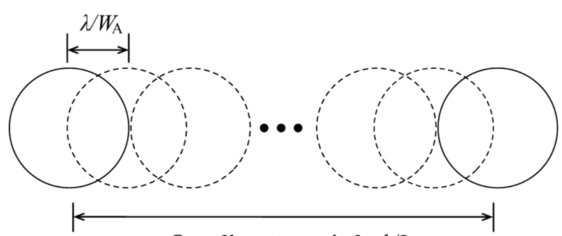

Fig. 3. Continuous scanning over one discrete period.

From Eq. (5), the precise offset (x_A) of the fiber tip in AFOC is the key to the continuous scanning. The distance between each scanning spots in Fig. 3 is $\frac{\lambda}{W_A}$, and the corresponding step length of x_A is:

$$sl = \frac{\theta_{\mathrm{as}}}{N-1}f_A = \frac{f_A}{W_A}\lambda \tag{12}$$

3. Experimental results and discussion

A prototype beam scanning device using a piezoelectric bimorph as the actuator is designed and the structural diagram is shown in Fig. 4. Continuous scanning can be achieved by driving piezoelectric bimorph to change the lateral offset of the fiber tip and the MLA simultaneously.

Corresponding experiment is performed to evaluate the performance of the proposed beam scanning system. The experimental arrangement of the proposed high-resolution beam scanning system is shown in Fig. 5. Two identical convex MLAs are used to form the Keplerian arrangement in the experiment. The width of exiting beam from the AFOC is limited by a square diaphragm with an appropriate size, so that the scanning spots can be adequately sampled in the CCD plane.

The experimental parameters are listed in Table 1. Accordingly, the angular separation and angular width are predicted to be 0.1815° and 0.0146° respectively.

When only MLAs are employed in the beam scanning system, the discrete scanning process in the angular range of 0° to 5° is obtained. Figure 7 in Appendix A shows the captured 28 scanning spots on a scan line. Without loss of generality, take one angular separation as an

Optics EXPRESS

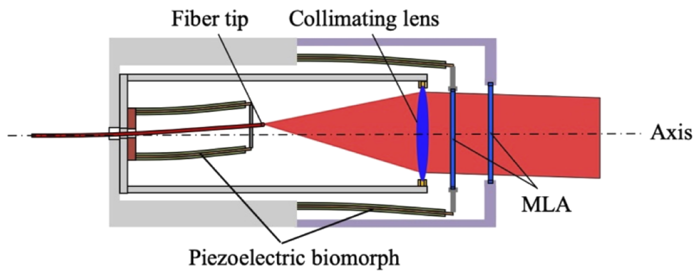

Fig. 4. Schematic diagram of the prototype device using piezoelectric bimorph as the actuator.

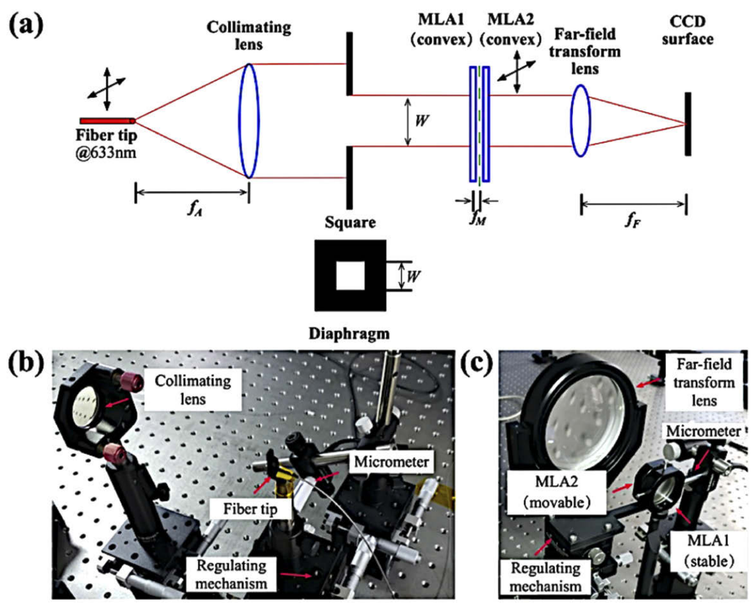

Fig. 5. The optical arrangement of the proposed beam scanning system. (a) Experimental arrangement. (b) Picture of AFOC component. (c) Picture of MLAs component.

Table 1. Parameters of AFOC-MLAs based beam scanning system used in the experiment

MLA	Micro lens width	200 µm	Far-field lens	Focal length	40 cm
	Fill factor	1	CCD camera	Brand	Spiricon
	Aperture	Φ3 cm		Model	L11059
	Focal length	1000 µm		Pixel size	9 µm
AFOC	Focal length	150 mm		Active area	35 mm×24 mm
	Fiber style	Single mode	Diaphragm	Shape	Square
	Wave length	633 nm		Width	0.5 cm

Optics EXPRESS

example to compare the scanning performance of the beam scanning systems employing only MLAs and that employing both MLAs and AFOC. According to Eq. (10), one angular separation can accommodate 26 scanning spots in the experiment with the scanning with both MLAs and AFOC, while only 2 scanning points can be accommodated in the system with only MLAs. From Eq. (12), x_A moves in a step of 19 μm, which updates x_M according to Eqs. (7) and (8). (Limited by the accuracy of the regulating mechanism, fine adjustments can be made to f_A, but only rough adjustments can be made to x_M). Figure 6(a) and (b) show the simulation and corresponding experimental results of the discrete scanning and continuous scanning in one angular separation, respectively. The results show that both theoretical simulations and experimental results are in good agreement, demonstrating the continuous scanning capacity of the beam scanning system employing both MLAs and AFOC. From the beam profiles shown in Fig. 6(b), it is also noticed that the diffraction limited performance is achieved in the continuous scanning. It is worth mentioning that similar to the beam scanning system employing only MLAs, the angular scanning range of the AFOC-MLAs based scanning system is also from 0° to 5°.

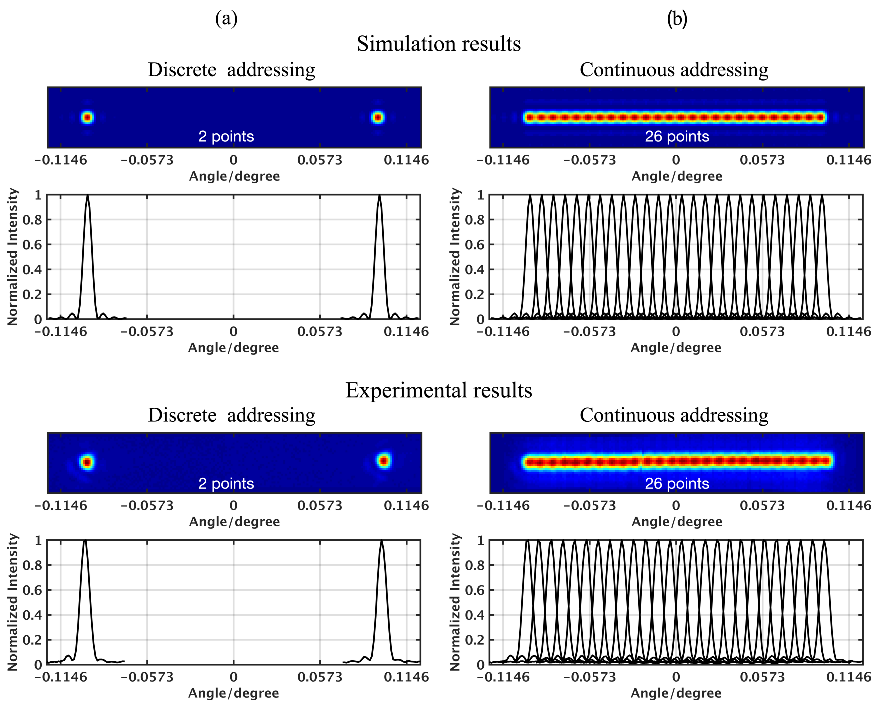

Fig. 6. Long-exposure captures of the line scanning: (a) MLAs produces discrete scanning in one discrete period; (b) AFOC-MLAs produces continuous scanning in one discrete period with diffraction limit resolution. The number of scanning spots increased from 2 to 26, covering the whole discrete period.

4. Conclusion

In summary, to address the discrete scanning issue of the beam scanning system with only MLAs, a solution using AFOC as a pre-scanning device was proposed and experimentally demonstrated. Continuous scanning with diffraction limit resolution (0.0146°) was achieved by the proposed beam scanning system employing both MLAs and AFOC. This method is also suitable for solving the discrete scanning problem of other scanning devices worked as blazed grating. The prototype device with piezoelectric bimorph as the actuator was technically demonstrated. Compared

Optics EXPRESS

with the traditional mechanical scanning devices, the proposed system has a smaller size, a more compact structure and a faster response speed. It is believed that this proposed beam scanning technique can find wide applications in the fields of optical communications, optical interconnection, power projection, coherent beam combining, and others.

Optics EXPRESS

Appendix A

Discrete scanning process in the field of view from 0° to 5°.

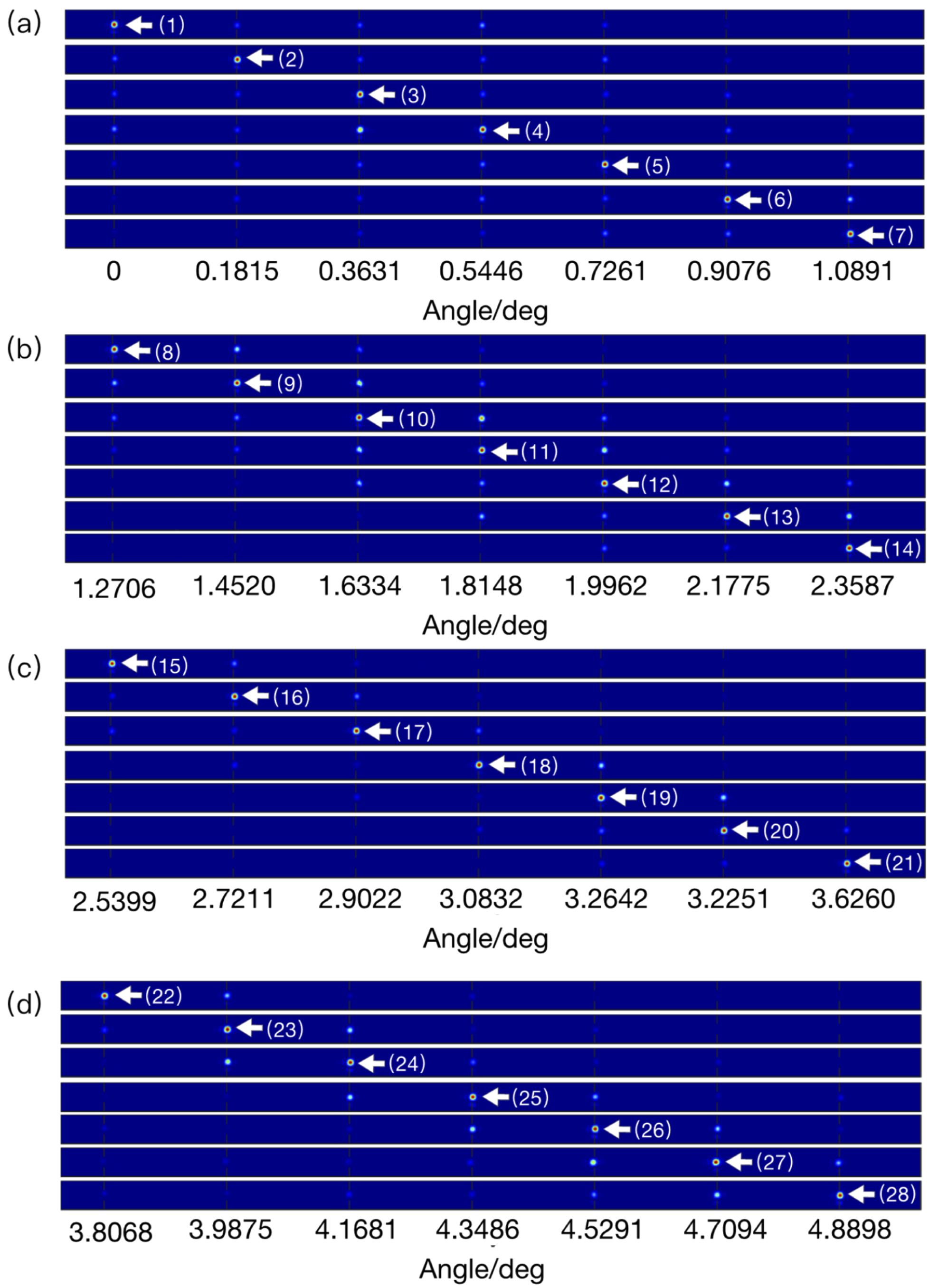

Fig. 7. Experimental far field views of the MLAs discrete scanning process.

Funding. National Natural Science Foundation of China (61675205).

Acknowledgments. The authors thank Axiu Cao, Yongfeng Zhang, and Xiangyu Wang for the fruitful discussions.

Disclosures. The authors declare no conflicts of interest.

References

1. P. F. McManamon, P. J. Bos, M. J. Escuti, J. Heikenfeld, S. Serati, H. Xie, and E. A. Watson, "A review of phased array steering for narrow-band electrooptical systems," Proc. IEEE **97**(6), 1078–1096 (2009).
2. S. A. Miller, Y. C. Chang, C. T. Phare, M. C. Shin, and M. Lipson, "Large-scale optical phased array using a low-power multi-pass silicon photonic platform," Optica **7**(1), 3 (2020).
3. W. S. Rabinovich, P. G. Goetz, M. W. Pruessner, R. Mahon, M. S. Ferraro, D. Park, E. Fleet, and M. J. Deprenger, "Free space optical communication link using a silicon photonic optical phased array," Proc. SPIE **9354**, 93540B (2015).
4. W. C. Goltsos and M. Holz, "Agile beam steering using binary optics microlens arrays," Opt. Eng. **29**(11), 1392–1397 (1990).
5. J. L. Gibson, B. D. Duncan, E. A. Watson, and J. S. Loomis, "Wide-angle decentered lens beam steering for infrared countermeasures applications," Opt. Eng. **43**(3), 568–2321 (2004).
6. A. Akatay and H. Urey, "Design and optimization of microlens array based high resolution beam steering system," Opt. Express **15**(8), 4523–4529 (2007).
7. S. K. Gokce, S. Holmstrom, C. Hibert, S. Olcer, D. Bowman, and H. Urey, "Two-dimensional MEMS stage integrated with microlens arrays for laser beam steering," J. Microelectromech. Syst. **20**(1), 15–17 (2011).
8. D. Krogmann and H. D. Tholl, "Infrared micro-optics technologies," Proc. SPIE **5406**, 121–132 (2004).
9. C. Geng, F. Li, J. Zuo, J. Liu, X. Yang, T. Yu, J. Jiang, and X. Li, "Fiber laser transceiving and wavefront aberration mitigation with adaptive distributed aperture array for free-space optical communications," Opt. Lett. **45**(7), 1906–1909 (2020).
10. G. Huang, C. Geng, F. Li, Y. Yang, and X. Li, "Adaptive SMF Coupling Based on Precise-Delayed SPGD Algorithm and Its Application in Free Space Optical Communication," IEEE Photonics J. **10**(3), 1–12 (2018).
11. F. Li, C. Geng, G. Huang, Y. Yang, X. Li, and Q. Qiu, "Experimental Demonstration of Coherent Combining With Tip/Tilt Control Based on Adaptive Space-to-Fiber Laser Beam Coupling," IEEE Photonics J. **9**(2), 1–12 (2017).
12. Y. Yang, C. Geng, F. Li, G. Huang, and X. Li, "Multi-aperture all-fiber active coherent beam combining for free-space optical communication receivers," Opt. Express **25**(22), 27519–27532 (2017).
13. S. Glockner and R. Goring, "Analysis of a micro-optical light modulator," Appl. Opt. **36**(7), 1467–1471 (1997).
14. J. W. Goodman, *Introduction To Fourier Optics* (1995).